Molten Salt Synthesis of Iron Oxide Modified Attapulgite for Catalytic Oxidation of Elemental Mercury

[1,2] Yu Lu, [1] Jing Ling Shao, [1] Hui Cang, [1] Fen Nv Han, [2] Zhi Dong Chen and [1] Qi Xu*

[1] *College of Chemical Engineering and Biological, Yancheng Institute of Technology, Yancheng 224051, China.*

[2]*School of Petrochemical Engineering, Changzhou University, Changzhou 213164, China.*

xqsteve@ycit.cn*

(Received on 13th July 2012, accepted in revised form 12th November 2012)

Summary: Iron oxide modified attapulgite (Fe_2O_3-ATP) catalysts, with special network structure, was prepared by molten salt method, and was applied to investigate Hg^0 oxidation ability in simulated flue gas from 100 to 260°C. Scanning electron microscopy (SEM), X-ray diffraction (XRD) and Fourier-transform infrared (FTIR) spectroscopy were employed to characterize the catalysts. The results showed that Fe_2O_3-ATP exhibited about 90% average Hg^0 oxidation efficiency at 220°C. With the decrease of the Fe_2O_3 in Fe_2O_3-ATP, the Hg^0 oxidation efficiency reduced. Furthermore, the flue gas components seriously affected the Hg^0 oxidation. The presence of Cl_2 and O_2 could promote the Hg^0 oxidation, while SO_2 would inhibit Hg^0 oxidation. Cl_2 was the most effective component of the three for Hg^0 oxidation.

Keywords: Fe_2O_3-ATP, Hg^0, SEM, XRD, FTIR.

Introduction

The pollution of trace metal, especially mercury, in coal-fired flue gas has aroused wide concern. Due to its high toxicity, strong volatility, and lasting stability, mercury is poisonous to both human and animals. There exists three forms of mercury in coal-fired flue gas: elemental(Hg^0), oxidized(Hg^{2+}), and particulate(Hg(p)) [1]. Among them, Hg(p) and Hg^{2+} are easier to be removed than Hg^0. Hg(p) can be captured by existing air pollution control devices such as electrostatic precipitators (ESP) and bag dust collector. Hg^{2+} can be removed by wet flue gas desulfurization (FGD) due to its water solubility. In contrast, Hg^0 can't be removed by FGD because it is almost insoluble in water. Consequently, if Hg^0 could be oxidized to water-soluble Hg^{2+} by catalytic oxidation of catalysts, it will have important significance for the control of mercury emission in coal-fired flue gas.

Currently, several metal oxides such as Fe_2O_3 [2], CeO_2 [3], Mn_2O_3 [4], CuO [5] and V_2O_5 [6] have been demonstrated to have oxidation activities toward Hg^0, especially at relative low temperatures. Among the above catalysts, Fe_2O_3 has the advantages of abundance, strong toxicity resistance and inexpensive. However, the pure Fe_2O_3 catalysts are harmful to the environment, and its catalytic activity is not high. By using attapulgite as carrier, Fe_2O_3 is uniformly dispersed on the surface of attapulgite for preventing agglomeration, and enhancing catalyst activity.

Attapulgite (ATP) is a natural nano-structural hydrated magnesium aluminum silicate with 1-D fibrillar morphology [7], which has large surface area and zeolite-like channels, and can be used as absorbent, catalyst and catalyst support [8-11]. At low temperature, through adsorptive effect, the average Hg^0 removal efficiency of $CuCl_2$-impregnated ATP reached about 90% [12]. At present, the methods of metal modified ATP mostly focus on impregnation, ion exchange, co-precipitation and sol-gel. These methods are complex and limited. Molten salt synthesis is one of the simplest ways to prepare oxides or complex oxides. When the temperature is above the melting point of the salts, the liquid phase is formed to be used as reaction medium or promoter [13-15] This method enables shorter reaction time and lower formation time because of the high diffusivities of the components, moreover it can control the particle morphology and stabilize different polymorphs [14].

In this work, the netting-shaped iron oxide modified attapulgite (Fe_2O_3-ATP) catalysts were synthesized by molten salt method. The study focused on the preparation of catalysts, the effects of Fe_2O_3/ATP ratio, reaction temperature and individual flue gas components for Hg^0 oxidation efficiency.

Results and Discussion

Catalysts Characteristics

Fig. 1 presents the SEM images of ATP (calcined at 500°C), Fe_2O_3(molten salt method) and

*To whom all correspondence should be addressed.

Fe_2O_3-ATP(2:1) respectively. As shown in Fig. 1a and 1b, ATP showed the long and narrow fiber-shape [16], and Fe_2O_3 displayed the disordered sheeted structure. However, after synthesizing Fe_2O_3-ATP(2:1) by molten salt method, the Fe_2O_3 sheets aggregated together orderly forming netting(Fig. 1c, 1d), and no special fiber structure of ATP existed, which might be due to Fe_2O_3 was widely dispersed on the ATP surface. It's propitious to increase the active sites on catalysts for mercury oxidation.

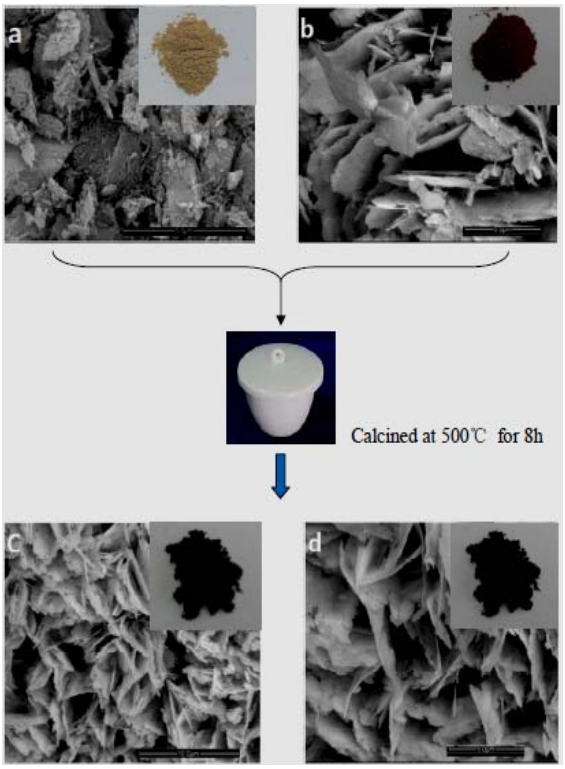

Fig. 1: SEM images of ATP (calcined at 500°C), Fe_2O_3 (molten salt method) and Fe_2O_3-ATP(2:1).

The XRD patterns of ATP(calcined at 500°C), Fe_2O_3-ATP(1:1) and Fe_2O_3-ATP(2:1) are shown in Fig. 2. The typical diffraction peaks at 2θ=19.96°, 27.58° were corresponding to the primary diffraction of the (040) and (400) planes for ATP [17,18], which could be detected in the X-ray diffraction pattern of ATP and Fe_2O_3-ATP(1:1). However, these characteristic peaks of ATP weren't found over Fe_2O_3-ATP(2:1), which indicated that Fe_2O_3 was highly dispersed on the surface of ATP. The peaks at 2θ=33.14°, 35.60°, 49.40° and 54.26° ascribed to the specific peaks of Fe_2O_3, which could also demonstrate that Fe_2O_3 had dispersed on the ATP surface for both Fe_2O_3-ATP(1:1)and Fe_2O_3-ATP(2:1).

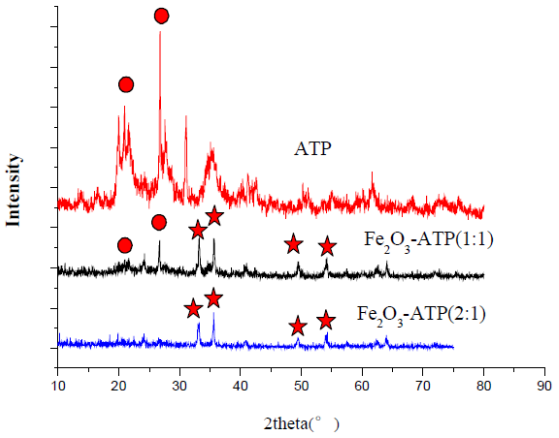

Fig. 2: XRD patterns of ATP(calcined at 500°C), Fe_2O_3-ATP(1:1) and Fe_2O_3-ATP(2:1).

Fig. 3 shows the FT-IR results of ATP(calcined at 500°C), Fe_2O_3, Fe_2O_3-ATP (1:1) and Fe_2O_3-ATP (2:1) composite material. It was observed that the FT-IR spectra of Fe_2O_3-ATP (1:1) and Fe_2O_3-ATP (2:1) are almost the same. The absorbance bands at 463.74cm^{-1} and 573.16cm^{-1} ascribed to the symmetry and asymmetry stretching vibration of Fe-O [19], which colud be detected in the curves of Fe_2O_3, Fe_2O_3-ATP(1:1) and Fe_2O_3-ATP (2:1). After adding ATP, a new band at 1029.07cm^{-1} of Si-O characteristic peak for ATP emerged in the FT-IR spectrum of Fe_2O_3-ATP (1:1) and Fe_2O_3-ATP (2:1). The result indicated that Fe_2O_3 had successfully dispersed on the ATP surface. The result was in compliance with the result of Fig. 1 and Fig. 2.

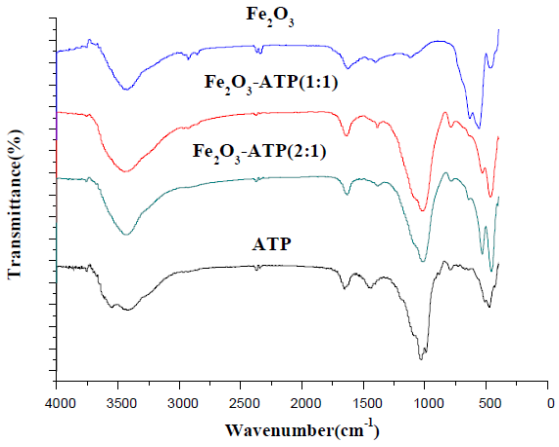

Fig. 3: FT-IR spectra of ATP(calcined at 500°C), Fe_2O_3, Fe_2O_3-ATP(1:1) and Fe_2O_3-ATP(2:1).

The wide and strong absorbance bands at 3424.38cm^{-1} and 1632.73cm^{-1} were corresponding to the stretching and bending vibrations of the absorbed water.

Catalytic Activity

Hg^0 oxidation efficiency over ATP(calcined at 500°C), Fe_2O_3(molten salt method), Fe_2O_3-ATP(1:1) and Fe_2O_3-ATP(2:1) at various temperatures is displayed in Fig. 4. It was observed that the Hg^0 oxidation efficiency improved remarkably for Fe_2O_3-ATP (2:1), which presented approximate 90% oxidation efficiency at 220°C. Nevertheless, with the decrease of Fe_2O_3, the activity of Fe_2O_3-ATP(1:1) for Hg^0 oxidation obviously reduced. In this process, the adsorption of Hg^0 by ATP played the leading role, because ATP wasn't completely coated by Fe_2O_3. Almost no obvious Hg^0 oxidation was observed over pure ATP, the Hg^0 oxidation efficiency was less than 5%. However, the Hg^0 removal efficiency of ATP could reach to 10% through adsorption mainly. The adding of Fe_2O_3 provided more surface chemisorbed oxygen, and the special network structure supplied more active sites for Hg^0 oxidation. For all catalysts above, the Hg^0 oxidation efficiency enhanced when temperature was from 100 to 220°C, and with the continued increase of the temperature to 260°C, the Hg^0 oxidation efficiency decreased.

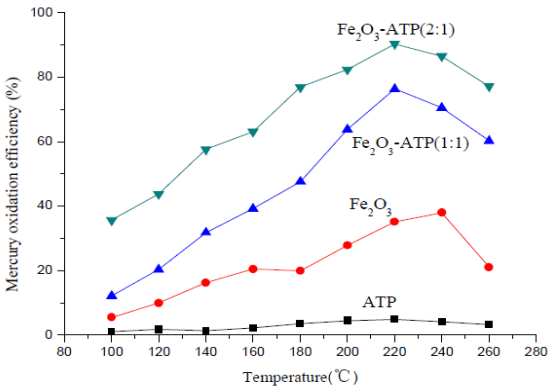

Fig. 4: Effect of the temperature on Hg^0 oxidation.

Effect of O_2, Cl_2 and SO_2 on Hg^0 OxidationEfficiency

To better understand the Hg^0 oxidation capacity of Fe_2O_3-ATP(2:1), it's necessary to discuss the effect of individual flue gas components on Hg^0 oxidation efficiency, especially O_2, Cl_2 and SO_2. The experiments were examined at 220°C.

The average Hg^0 oxidation efficiency of different O_2 content (0, 6%, 12%) in simulated flue gas is shown in Fig. 5. With the increase of O_2, Hg^0 oxidation efficiency rose slowly. Under the absence of O_2, Hg^0 oxidation efficiency was about 24.8%. When the concentration of O_2 was up to 6%, no obvious increase was observed, and only about 29.7% of Hg^0 was oxidized even if the concentration is increased to 12%. The results revealed that the Fe_2O_3-ATP(2:1) possessed large oxygen storage capacity and consumed only a small part of the stored oxygen in mercury oxidation [3]. Cl_2 has promotional effect for Hg^0 oxidation due to $HgCl_2$ was the main oxidized mercury species in coal combustion flue gas [20]. As described in Fig. 6, the impacts of Cl_2 were researched in the range of 0-50ppm. Comparing with O_2, Hg^0 oxidation ability in the present of Cl_2 enhanced largely. When the concentration of Cl_2 was transferred from 0 to 50ppm, the Hg^0 oxidation efficiency of Fe_2O_3-ATP(2:1) was enhanced from 32.5% to 93.2%. Whereas, as the Cl_2 continued to increase, no evident increase of Hg^0 oxidation efficiency was detected. Impeditive effect of SO_2 on Hg^0 oxidation over Fe_2O_3-ATP(2:1) was summarized in Fig. 7. When SO_2(400,800,1600ppm) was added into the simulated flue gas in the absence of O_2, almost no Hg^0 oxidation was observed. Hailong Li *et al* [3] studied the competition of Hg^0 and SO_2 for the active sites on catalysts, and the result illustrated that the affinity between SO_2 and catalyst was stronger than that between Hg^0 and catalyst. Therefore, the presence of SO_2 restrained the Hg^0 oxidation capacity of Fe_2O_3-ATP(2:1).

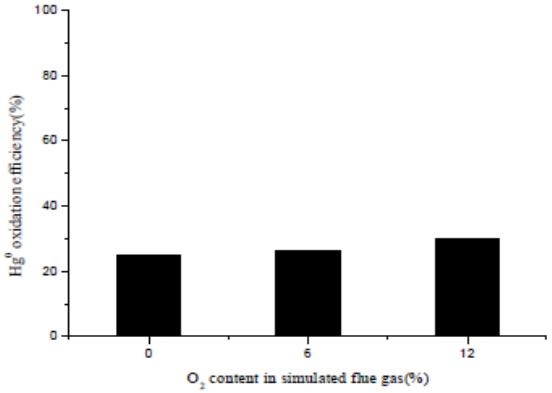

Fig. 5: Effect of O_2 on Hg^0 oxidation.

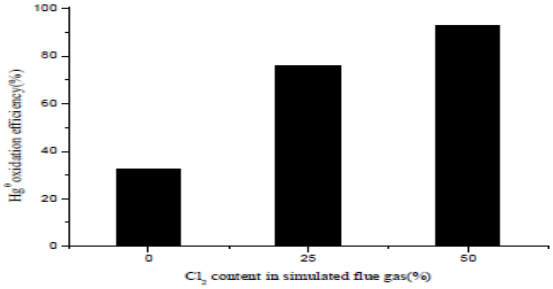

Fig. 6: Effect of Cl_2 on Hg^0 oxidation.

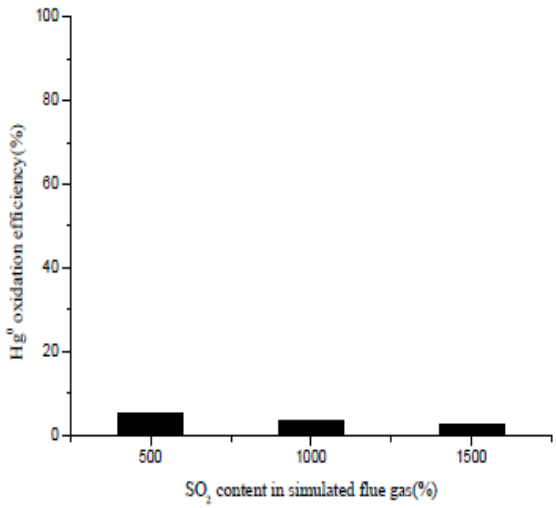

Fig. 7: Effect of SO_2 on Hg^0 oxidation.

Experimental

Catalysts Preparation

Attapulgite (ATP) was supplied by Jiangsu Dongda Heating and Mechanical Manufacture Company(China). Hydrochloric acid (HCl), silver nitrate ($AgNO_3$), ferric nitrate ($Fe(NO_3)_3{\cdot}9H_2O$), sodium chloride (NaCl) and absolute ethyl alcohol (EtOH) used in this study were analytical grade.

ATP was firstly treated with 37% hydrochloric acid at 110ºC for 2h, followed by washing with distilled water until no Cl^- detected(tested with $AgNO_3$), and then dried at 80°C for 8 h before use.

The molten salt method was used to synthesize Fe_2O_3-ATP catalysts. 0.01mol $Fe(NO_3)_3{\cdot}9H_2O$, 0.1mol NaCl and the purified ATP(the mass ratio of ATP/$Fe(NO_3)_3{\cdot}9H_2O$ was 1:1 and 1:2, respectively) were mixed, and ground homogenously. The mixtures were heated to a target temperature of 500°C for 8 h, and then air-cooled. The products was thoroughly washed with 50% aqueous ethanol(v/v) at room temperature, and then dried overnight in air at 80°C.

Characterization of Catalysts

The catalysts were characterized by X-ray diffraction (DX-2700 diffractometer), using Cu Kα as radiation over the 2θ range of 10°~70°. SEM images were obtained by using QUANTA200 scanning electron microscope(FEI Company) to observe the morphology of catalysts. FTIR spectra of the samples were taken with NEXUS-670 FT-IR spectroscopy (NICOLET) in the range of 400-4000cm^{-1}.

Activity Tests

The apparatus used in this work is illustrated in Fig. 8. The catalytic oxidation activities of Hg^0 over Fe_2O_3-ATP were carried out in a fixed-bed flow reactor system under a total flow of 1L/min and a gas hourly space velocity(GHSV) of about 37700h^{-1}. In each experiment, 0.5g of the catalyst was placed in the fixed-bed reactor(13mm inner diameter) with temperature controlling from 100 to 260°C. The simulated flue gas was composed of 6% O_2, 12% CO_2, 300ppm NO, 1500ppm SO_2, 50ppm Cl_2, and balance gas N_2. The N_2 flow was distributed into two branches: one branch(100ml/min) passed through a Hg^0 permeation tube (QMG-6-6) to introduce the saturated Hg^0 vapor(20μg/m^3) into the simulated flue gas system, and the other branch converged with the individual streams of NO, CO_2, SO_2 and O_2, and formed the main gas flow. The gases were adjusted by mass flow controllers, and mixed, pre-heated before entering the reactor.

The Hg^0 concentrations at both the inlet and outlet of reactor were measured by the mercury analyzer (QM201H Hg^0 analyzer). After analysis, the exhaust gas must pass through the 0.1M $KMnO_4$ solution before being introduced into the air. However, the Hg^0 analyzer can only measure the concentration of Hg^0. Therefore, in order to measure the concentration of total mercury including Hg^0 and oxidized Hg^0, the $SnCl_2$ solution(the oxidized Hg^0 could be reduced to Hg^0 via the reducing action of $SnCl_2$ solution) was located between the fixed-bed reactor and the Hg^0 analyzer. The Hg^0 oxidation efficiency(η) was quantified by the difference of Hg^0 concentration after and before passing the $SnCl_2$ solution. The efficiency of Hg^0 oxidation over Fe_2O_3-ATP catalysts can be evaluated as follows:

$$\eta_{Hg\ oxi(\%)}=\frac{[Hg]_{total}-[Hg^0]}{[Hg]_{total}}$$

where $\eta_{Hg\ oxi(\%)}$ is the Hg^0 oxidation efficiency, $[Hg]_{total}$ is the concentration of total mercury after passing the $SnCl_2$ solution, and $[Hg^0]$ is the concentration of Hg^0 before passing the $SnCl_2$ solution.

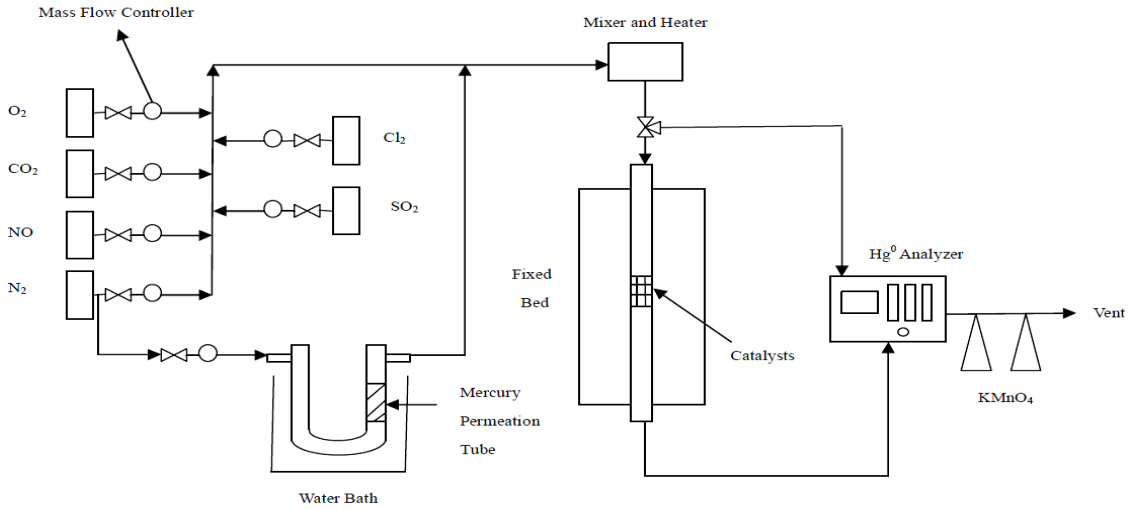

Fig. 8: Schematic diagram of fixed-bed reactor system.

Conclusion

In this work, the Hg^0 oxidation efficiency of Fe_2O_3-ATP catalysts were studied in a fixed-bed flow reactor system at 100-260°C. As a result, Fe_2O_3-ATP with special netting structure were effective catalysts for Hg^0 oxidation, the Hg^0 oxidation efficiency of Fe_2O_3-ATP(2:1) arrived about 90% at 220°C. The decrease of Fe_2O_3 would lessen the Hg^0 oxidation efficiency of Fe_2O_3-ATP. In addition, the flue gas components have significant effects to Hg^0 oxidation. Both O_2 and Cl_2 promoted Hg^0 oxidation ability of Fe_2O_3-ATP(2:1), especially Cl_2. When 50ppm Cl_2 was added, the Hg^0 oxidation efficiency reached 93.2%. However, SO_2 went against Hg^0 oxidation, almost no Hg^0 oxidation was discovered in the presence of SO_2 alone. In summary, Fe_2O_3-ATP were feasible catalysts for Hg^0 oxidation in flue gas.

Acknowledgements

This work was supported finanacially by the Open Project of Key Laboratory for Advanced Technology in Environmental Protection of Jiangsu Province(AE201026, AE201165), the Innovation Fund Project of Yancheng Institute Of Technology(YKB201106),

References

1. A. A. Presto and E. J. Granite. *Environmental Science and Technology*, **40**, 5601 (2006).
2. F. H. Kong, J. R. Qiu, H. Liu, R. Zhao and Z. H. Ai. *Journal of Environmental Sciences*, **23**, 699 (2011).
3. H. L. Li, C. Y. Wu, Ying Li and J. Y. Zhang. *Environmental Scencei and Technoogy*, **45**, 7394 (2011).
4. L. Ji, P. M. Sreekanth, P. G. Smirniotis, S. W. Thiel and N. G. Pinto. *Energy and Fuels*, **22**, 2299 (2008).
5. A. Yamaguchi, H. Akiho and S. Ito. Powder Technology, **180**, 222 (2008).
6. S. He, J. S. Zhou, Y. Q. Zhu, Z. Y. Luo, M. J. Ni and K. F. Cen. *Energy and Fuels*, **23**, 253 (2009).
7. Z. G. Chen, F. Chen, X. Z. Li, X. W. Lu, C. Y. Ni and X. B. Zhao. *Journal of Rare Earths*, **28**, 566 (2010).
8. J. You, F. Chen, X. B. Zhao and Z. G. Chen. *Journal of Rare Earths*, **28**, 347 (2010).
9. D. M. A. Melo, J. A. C Ruiz, M. A. F Melo, E. V. Sobrinho and A. E. Martinelli. *Journal of Alloys and Compounds*, **344**, 352 (2002).
10. B. Joy, S. Ghosh, P. Padmaja and M. Lalithambika. *Catalysis Communieations*, **6**, 573 (2005).
11. D. M. A. Melo, J. A. C Ruiz, M. A. F Melo, E. V. Sobrinhob and M. Schmall. *Microporous and Mesoporous Materials*, **38**, 345 (2000).
12. F. Ding, Y. C. Zhao, L. L. Mi, H. L. Li, Y. Li and J. Y. Zhang. *Industrial and Engineering Chemistry Research*, **51**, 3039 (2012).
13. Y. Zhang, L. Q. Wang and D. F. Xue. *Powder Technology*, **217**, 629 (2012).
14. H. L. Li, Z. N. Du, G. L. Wang and Y. C. Zhang. *Materials Letters*, **64**, 431 (2010).
15. J. Q. Lu, X. F. Wang, Y. T. Wu and Y. Q. Xu. *Materials Letters*, **74**, 200 (2012).
16. C. Catrinescu, D. Arsene and C. Teodosiu. *Applied Catalysis* B*: Environmental*, **101**, 451 (2011).
17. Y. S. Liu, P. Liu, Z. X. Su, F. S. Li and F. S. Wen. *Applied Surface Science*, **255**, 2020 (2008).
18. J. M. Xu, W. Li, Q. F. Yin and Y. L. Zhu. *Electrochim Acta*. **52**, 3601 (2007).
19. J. M. Pan, L. C. Xu, J. D. Dai, X. X. Li, H. Hang, P. W. Huo, C. X. Li and Y. S. Yan. *Chemical Engineering Journal*, **174**, 68 (2011).
20. B. Krishnakumar and J. J. Helble. *Environmental Science and Technoogy*, **41**, 7870 (2007).